# Thermal and hygroscopic study of hemp concrete in real ambient conditions

M. Asli, Emilio Sassine, F. Brachelet, Emmanuel Antczak

# Thermal and hygroscopic study of hemp concrete in real ambient conditions

M. ASLI[1], E. SASSINE[2]*, F. BRACHELET[1], E. ANTCZAK[1]

[1] Univ. Artois, Univ. Lille, Institut Mines-Télécom, Junia, ULR 4515 – LGCgE, Laboratoire de Génie Civil et géo-Environnement, F-62400 Béthune, France

[2] Lebanese University, Habitat and Energy Unit, Group of Thermal and Renewable Energies - Laboratory of Applied Physics (LPA-GMTER), Faculty of Sciences, Fanar Campus, Lebanon

*Corresponding author : emilio.sassine@gmail.com

**Abstract**

Most building materials, and more particularly bio-based materials, are subject to hygrothermal transfers in the environment in which they are disposed. These transfers depend on their thermophysical characteristics as well as the ambient humidity and temperature conditions. In such environment, and despite these variations, the material must be able to ensure in a sustainable manner, the functions for which it was implemented (thermal, mechanical, acoustic ...). Among these materials, hemp concrete, which is a bio-based material, is widely considered in building construction for its superior thermal and hygroscopic performance. The hygrothermal modelling of such materials in real conditions is essential for a better understanding of buildings' energy performances. Several works targeted the numerical hygrothermal modelling of hemp concrete; however most of them are done in controlled laboratory conditions, which may be different from the real buildings scenarios. In this paper, heat and mass transfer are investigated both numerically and experimentally in real conditions. The hygrothermal properties of hemp concrete were first determined through laboratory experiments; then, an experimental wall segment made of hemp concrete was instrumented in real ambient conditions in order to validate the Philip and De Vries model describing heat and mass transfer. The comparison of the numerical results to the experimental data leads to interesting results regarding local temperature and relative humidity variations. Moreover, numerical investigation of the moisture buffer values of hemp concrete was performed and the results were validated by bibliographic data. The hemp concrete was found to be a very interesting potential hygrothermal regulation material in terms of thermal conductivity, decrement factor, time lag, and humidity regulation.

**Keywords**

Hemp concrete, MBV, Thermal conductivity, Water vapor sorption, Numerical simulation, Heat and Mass Transfer, experimental facility, sensitivity analysis.

## 1 INTRODUCTION

The scientific community carried out several work in order to demonstrate the thermal and hygroscopic efficiency of bio-based material compared to classical insulation materials, and the advantages they offer in terms of energy needs [1], environmental impact [2], indoor air quality, durability [3], [4], [5], and thermal comfort [6].

Hemp concrete is one of the most famous bio-based materials, it offers an ecological alternative solution with advantageous thermal properties [7], [8], [9] and moisture buffering capacity [10], [11], with a low life cycle impact compared to similar products [12]. Numerous authors investigated the hygrothermal properties of hemp concrete. Elfordy et al. [13] assessed the impact of hemp concrete density on its thermal and mechanical properties. Collet et al. [10] determined experimentally the Moisture Buffer Value (MBV) of hemp concrete. Tran et al. [14] studied the impact of transient hygrothermal behavior of hemp concrete in building envelopes [14]. Lelievre et al. [15] investigated the hygrothermal behavior at different scales (sample and wall) and under various controlled conditions.

Furthermore, the positive effect of hemp concrete on building energy consumption was demonstrated in several works [14], [16], [17], [18]. Besides its impact on the energy consumption, the humidity in the building envelope can also lead to problems related to materials' durability and internal mold risks [19], [20]. For these reasons, it is essential to be able to precisely quantify heat and moisture transfers phenomena within construction building materials.

In the literature, numerous works deal with simultaneous heat and mass transfer within porous media. Several experiments assessing the hygrothermal behavior of bio-based materials such as wood fiber materials [21], [22], hemp concrete [10], [14], [23], [24] were performed at different scales (material sample, wall, and building). These experimental methods allow the assessment of water content, temperature, and relative humidity within the investigated media subjected to controlled boundary conditions and the results were used to validate the numerical models describing heat and mass transfer [15], [23]. Generally, good agreement is found between the numerical and measured data. Nevertheless, in most of the cases, the experiment is held in controlled temperature and relative humidity conditions and may not reflect accurately the hygrothermal behavior in real uncontrolled conditions where the simultaneous heat and mass transfer phenomena are more complex.

In this work, heat and mass transfer phenomena within hemp concrete submitted to real ambient conditions are studied through numerical and experimental approaches. In the numerical work, the model of Philip and De Vries [25] is adopted (section 2). The input parameters of the model are experimentally determined with respect to the temperature and moisture content (section 3). A comparison between the experimental and numerical data as well as a sensitivity study are presented in (section 4), aiming at evaluating the results accuracy of the model. The last part is dedicated to the investigation of the moisture buffering capacity of hemp concrete (section 5); in this part the humidity regulation properties of hemp concrete are demonstrated and validated with respect to data founded in the bibliography.

## 2 MATHEMATICAL MODEL

The energy and mass balances equations derived from the energy and mass conservation principles, are applied under the following assumption:

- *The mass transfer takes place through the material's openings;*
- *The material is assumed to be continuous, homogeneous and no chemical reaction occurs;*
- *Local thermodynamic equilibrium is assumed at every point of the material;*
- *The effect of gravity is considered negligible*
- *The total gas pressure is considered to be constant and equal to the atmospheric pressure;*
- *No air transfer occurs;*
- *Liquid mass transfers under thermal gradients are neglected.*

Several models based on the previous assumption principles were provided by Luikov [26], Whitaker [27], Philip and De Vries [25], and adapted to building materials [28], [29]. The model of Philip and De Vries [25] is considered in this work for predicting the hygrothermal behavior of hemp concrete. This model considers that the moisture transport occurs under two phases (liquid and vapor); the vapor phase moves under a gradient of partial vapor pressure while the water phase moves under capillarity.

The model of Philip and De Vries is represented by Equations (1) and (2) describing mass and heat transfers respectively:

$$\frac{\partial \theta}{\partial t} = \frac{\partial}{\partial x}\left( D_\theta \frac{\partial \theta}{\partial x}\right) + \frac{\partial}{\partial x}\left( D_T \frac{\partial T}{\partial x}\right) \quad (1)$$

$$\rho_0 C_{pm} \frac{\partial T}{\partial t} = \frac{\partial}{\partial x}\left(\lambda \frac{\partial T}{\partial x}\right) + \rho_l L_v \left( \frac{\partial}{\partial x} D_{T,v} \frac{\partial T}{\partial x}\right) + \rho_l L_v \frac{\partial}{\partial x}\left(D_{\theta,v} . \frac{\partial \theta}{\partial x}\right) \quad (2)$$

Where θ is the water content and is expressed [kg.kg$^{-1}$], T is the temperature [°C], $D_T$ [m$^2$.s$^{-1}$K$^{-1}$], and $D_\theta$ [m$^2$.s$^{-1}$] are respectively, the mass transport coefficients associated to temperature and moisture content gradient.

$\rho_0$ is the dry density, $L_v$ is the latent heat of vaporization is set at 2500 KJ.kg$^{-1}$, $\rho_l$ represents the water density 1000 kg.m$^{-3}$, and $C_{pm}$ is the specific heat and is calculated as the average specific heat of solid matrix and liquid phase:

$$C_{pm} = C_{p0} + C_{pl} \frac{\rho_l}{\rho_0} \theta \quad (3)$$

λ is the equivalent thermal conductivity of the material and it is a function of moisture content. $D_{T,v}$ and $D_{\theta,v}$ are the vapor phase transport coefficients associated with temperature and moisture content gradient, respectively.

The associated boundary conditions are given by the equations (4) and (5), the index of the external and internal sides, respectively (x = 0, x = L).

$$-\lambda \nabla T - \rho_l L_v D_{T,v} \nabla T + \rho_l L_v D_{\theta,v} \nabla \theta = h_{T,L,0}\left(T_{a,e,i} - T_{s,e,i}\right) + \rho_l L_v\left(\rho v_{a,e,i} - \rho v_{s,e,i}\right) + \varphi_{rad,e,i} \quad (4)$$

Where $h_{T,L,0}$ is the convective heat transfer coefficient from external and internal sides, $\rho_{v,e,i}$ is the air density, and $\varphi_{rad,e,i}$ is a radiation term which is assumed negligible in our study.

The subscripts “e” and “I” correspond to external and internal sides respectively, and “a” and “s” correspond to air and solid surface neighboring environments respectively.

$$\rho_l \left( D_T \frac{\partial T}{\partial x} + D_\theta \frac{\partial \theta}{\partial x} \right) = h_{m,e,i} \left( \rho_{v,a,e} - \rho_{v,s,e} \right) \quad (5)$$

Where $h_{m,e,i}$ is the convective mass coefficients. To be closer to the reality, boundary conditions must be more realistic, otherwise the boundary conditions most relate the microscopic material properties with externals ambient variations. For this purpose, the temperature and relative humidity are measured during the test at the wall interface.

The relationships that relate transport coefficients of mass with transport coefficients of vapor and liquid phase are:

$$D_T = D_{T,l} + D_{T,v} \quad [m^2.s^{-1}K^{-1}] \quad (6)$$

$$D_\theta = D_{\theta,l} + D_{\theta,v} \quad [m^2.s^{-1}] \quad (7)$$

The diffusion coefficients are the most important factors used in the mathematical model, while the use of the experimental ways is required, so a great attention is paid to these coefficients. For this purpose the vapor diffusion coefficients are determined according to Zeknoun et al **[30]**, and Maalouf et al **[23]**. The transport coefficients associated with moisture gradient are related to water vapor permeability $\delta_0$ and the specific hygroscopic capacity ξ, which is the slope of sorption curve:

$$D_\theta = \frac{\delta_0 \ P_{v,s}}{\rho_0} \ \frac{1}{\xi} \quad (8)$$

$$\delta_0 = \frac{\delta_a}{\mu} \quad (9)$$

Where $\delta_a$ is the vapour permeability to air and it is equal to $2.10^{-10}$ $kg.m^{-1}.s^{-1}.Pa^{-1}$, μ is the water vapor resistance factor.

Vapor and liquid transport coefficients under a temperature gradient are given by the relations:

$$D_{T,v} = \frac{\delta_0 \ \varphi}{\rho_l} \ \frac{dP_{v,s}}{dT} \quad (10)$$

$$D_{\theta,l} = \frac{P_{vs}.\delta_p}{\xi_\varphi} \left( \frac{1}{\mu^*(\varphi)} - \frac{1}{\mu_0} \right) \quad (11)$$

μ* (ϕ) is the coefficient of water vapor resistance measured at high relative humidity, $\mu_0$ is the coefficient of water vapor resistance corresponding to the beginning of the capillary condensation.

## 3 MATERIAL CHARACTERIZATION

The studied hemp concrete sample is shown is Fig.1, it is a 20 cm x 30 cm x 60 cm block and manufactured by CHANVRIBLOC (La Mure, France) [31]. shows the manufactured hemp concrete block.

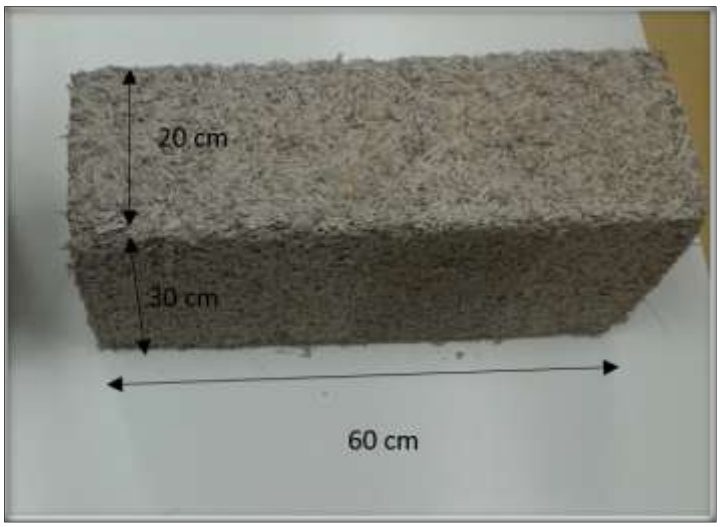


*Fig.1 Block of hemp concrete*

In order to guarantee the accuracy of the input parameters in the model, the material properties were measured in the laboratory.

The thermal conductivity was measured according to standard NF EN 12664 [32] under transient conditions on a sample of 400x400 mm, using fluxmeter of size 250x250mm. First, the sample is dried in a climatic chamber at 50°C and medium ventilation for a long duration in order to ensure that the humidity has been completely evacuated. The sample was weighed several times in order to check its stability by making sure that weight does not vary more than ± 2% of its mass. Afterwards, the same sample was moistened at different water content levels and weighed in the same way and the conductivity test is repeated by following the same protocol. In this way the curve in Fig. 2 was drawn, showing the evolution of the measured thermal conductivity of hemp concrete versus its water content. A dry thermal conductivity value of 0.07 $W.m^{-1}.K^{-1}$ is computed.

By using the same protocol, the heat fluxes were explored in order to determine the volumetric heat (ρc) as a function of the water content. The dry specific heat ($c_{p,s}$) was first determined, and then the evolution of volumetric heat capacity (ρc) versus the water content is investigated and reported in Fig.3.

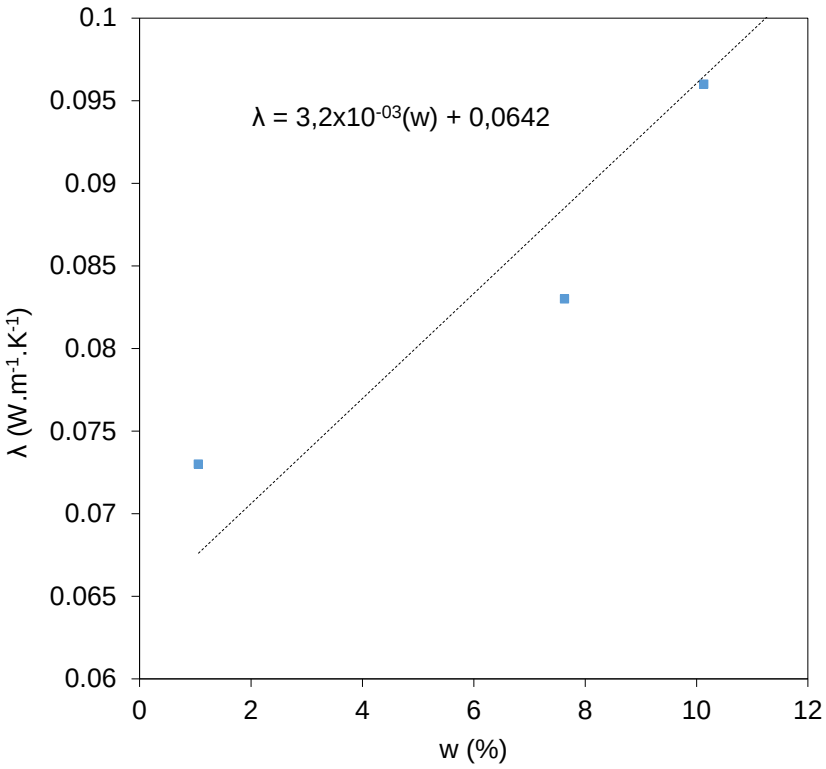


*Fig.2 Thermal conductivity of hemp concrete versus water content*

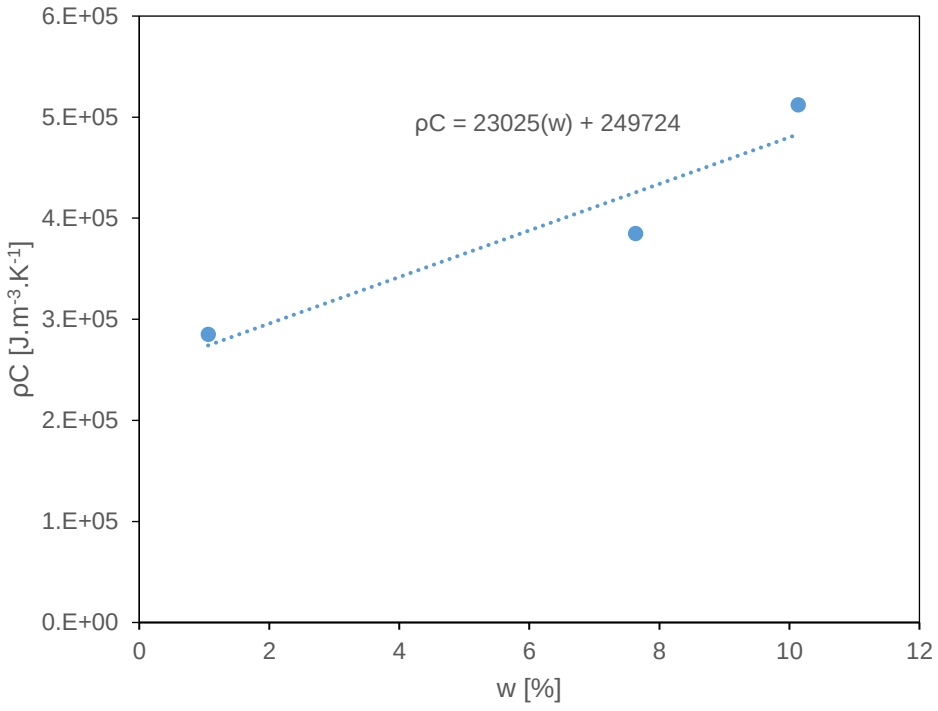


*Fig.3 Volumetric heat of hemp concrete versus water content*

The main sorption isotherms were determined at 23°C using a climatic chamber in order to reproduce relative humidity. Fig. 4 shows the experimental results obtained for the main adsorption and desorption isotherms of hemp concrete. The sorption desorption curves were determined according to the ISO 12571 standard [33], the test consists of placing samples in a climatic chamber under controlled conditions T and W, we vary the relative humidity between 0 and 100% while keeping the temperature constant, for at each relative humidity step the samples are weighed, and so the water content is determined for each relative humidity step. The experimental data are fitted with a GAB model [34], [35], which assumes a mono and multi-layer moisture adsorption at the pore surface. The GAB model is considered to be among the most efficient for this purpose and can be used to approximate the experimental data for water activity up to 0.9 presented in the form:

$$w = \frac{C.\ \theta_m.K.\ RH}{(1 - K.\ RH).\ (1 - K.\ RH + K.C.RH)} \quad (12)$$

Where $\theta_m$, C and K are the fitting coefficients (-). In the studied case, $\theta_m$ = 0.034, C = 165.64 and K = 0.834 for the main adsorption curve and $\theta_m$ = 0.042, C = 275.54 and K = 0.78 for the main desorption curve. The measurements and fitted curves for the adsorption and desorption isotherms of hemp concrete are shown in Fig. 4.:

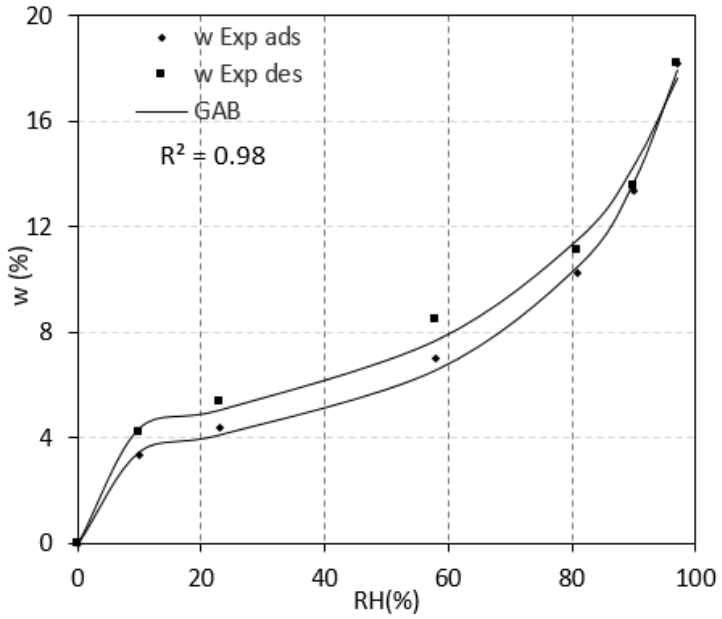


*Fig.4 Main adsorption and desorption isotherms of hemp concrete: measurements and fitted curves.*

The water vapor permeability is a hygrothermal parameter correlated to the water vapor resistance μ, where μ was carried out according to standard NF EN ISO 12572 [36]. The test is based on the cup method to determine the water vapor resistance of materials under isothermal conditions. This test consists in imposing a permanent and unidirectional vapor pressure gradient on a sample of given thickness. The vapor pressure gradient is obtained by placing a saline solution on the underside of the sample to reproduce $HR_{int}$. A saturated solution of sodium hydroxide (NaOH) was used in order to obtain a very low relative humidity (0% -2%) inside the cup. The effectiveness of this solution was tested

beforehand by placing it in a sealed cup with a humidity sensor; very satisfactory results were obtained where the relative humidity did not exceed the 2%. The used cups are made of glass and are therefore watertight, in order to comply with the device described in the standard on the one hand, and to avoid corrosion on the other hand. The sealant used is paraffin because it is impermeable to water vapor and does not undergo any chemical or physical transformation during the test.

The assembly consisting of the material to be tested and the cup + saline solution system is placed in a climatic chamber regulated in temperature and humidity where the external environment $HR_{ext}$ is reproduced. Since the behavior of hemp concrete is studied in real conditions, where the relative humidity varies between 0% and 100%, then the resistance to water vapor diffusion was investigated in this range to make the modeling as accurate as possible. Unfortunately, while studying the resistance to water vapor diffusion between 0-100%, it was found that working at high relative humidity > 85% leads to condensation phenomena which may distort the results. For that, the results were presented for RH varying between 0% and 80%.

Fig. 5 shows the principle of this test. The vapor flow is deduced from the variation in mass of the sample-cup assembly as a function of time.

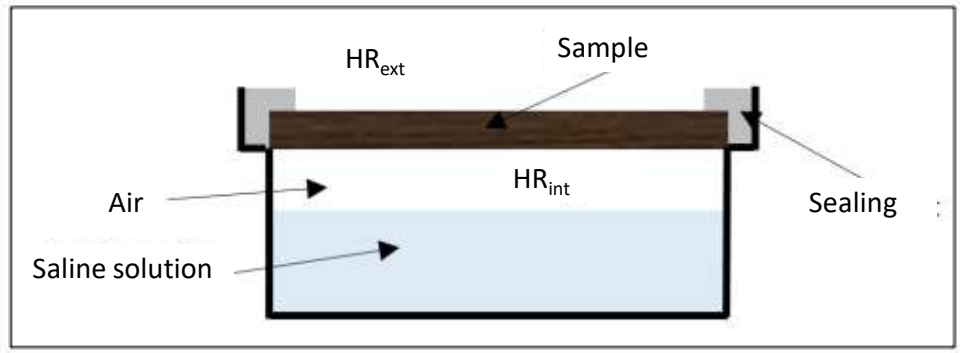


*Fig.5 Schematic view of the cup method*

Three samples were used according to the recommendation of standard NF EN ISO 12572 [36]. The following table summarizes the dimensions and the test protocol.

Table 1- Summary data for the water vapor permeability test

| Material | Boundary conditions | Exposed area (m x m) | Thickness (m) | $\mu_0$ [-] | $\mu^*$ |
|---|---|---|---|---|---|
| *Hemp concrete* | *RH : 0% - 80%*<br>*T : 23°C* | *0,175 x 0,175* | *0.04* | 10 | *3.72* |

The value found from this experimental protocol for hemp concrete is $\mu^* = 3.72$; this value is very close to that found by F. Collet et al [10].

## 4 INVESTIGATION OF THE SAMPLE IN REAL WEATHER CONDITIONS

### 4.1 Experimental setup

In order to evaluate the hygrothermal behavior of hemp concrete under real ambient conditions, a wall segment made of hemp concrete was instrumented and submitted to uncontrolled ambient temperature and relative humidity.

The sample of hemp concrete had already been investigated in previous studies [14] [37] [38] under controlled conditions; however, in the present study, the sample behavior under moderate changes of relative humidity and temperature inside a room/building is tested.

The tested sample has a large open surface (300×300 $mm^2$) and a thickness of 80 mm which is thicker than the moisture penetration depth calculated for such a material [10]. A smaller thickness causes measurement errors, while the large thicknesses of this material will not be representative of the reality; in real renovation applications, the projected thicknesses varies between 6 and 10 cm.
The sample was cut carefully with a jigsaw fixed on a table, the saw is connected to a mechanical arm for a better precision (one millimeter). The cut block was stored under laboratory conditions with an average temperature of 20°C and a relative humidity of 50% RH before inserting it within the wall.

The experiments were performed in the laboratory, where the sample (wall segment) was placed integrated to wall inside the ventilation opening as shown in Fig.6.

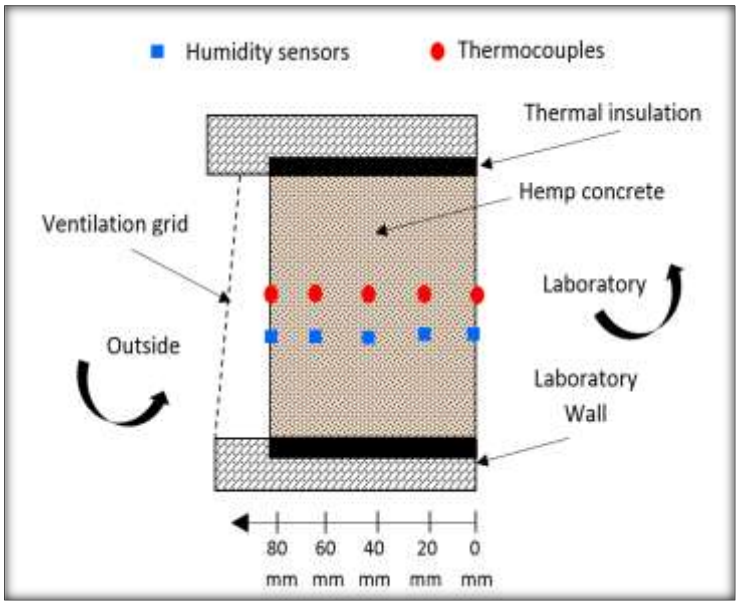


*Fig.6 Diagram of the experimental device.*

The sample was stored at 23°C and RH 50% for 15 days to get constant and known initial conditions. Additionally, all the sample lateral surfaces were insulated with silicone to ensure 1D heat and moisture transfer within the sample. The temperature and relative humidity were recorded at different positions within the wall segment (Fig.6). A particular care was accorded to the sensors installation on the faces and within the sample where three holes were perforated inside the wall segment every 20 mm, for positioning the temperature and humidity sensors. Indeed, due to the sample thickness, using less

sensors would lead to less precision while using more sensors would lead to measurement bulk. The authors found that the optimal solution would be to put a sensor every 20 mm in order to have the minimum influence between the sensors. Two additional sensors were used for evaluating the boundary conditions. The impact of sensors position accuracy will be investigated by sensitivity analysis, considering the heterogeneity of the material, this approach is necessary.
The five thermocouples with a diameter d = 0.2 mm and five humidity sensors HIH-4000 with a dimension (4.17 x 8.59 mm) used for this purpose (Fig.7), present many advantages such as having long-term stability and being individually calibrated; their accuracy is evaluated by the supplier (± 3.5% for humidity and ± 0.02 °C for temperature).

The data recorded through a data acquisition system GL820 [39] connected to all the sensors, and the monitoring lasted two month with a time step of five minutes (300 s).

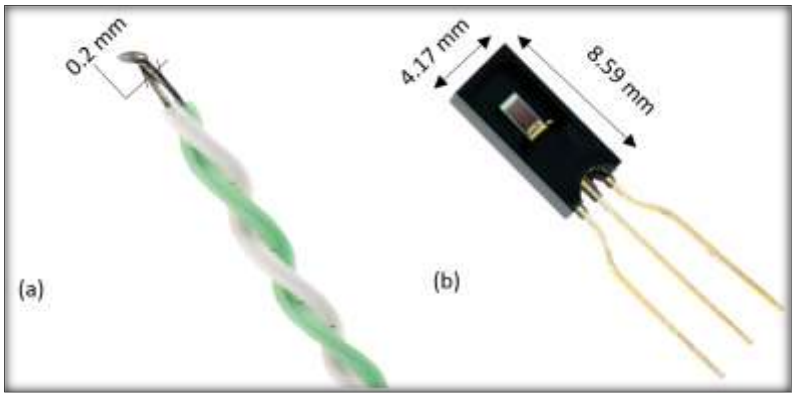


*Fig.7 Themocouple (a) and humidity sensor HIH-4000 (b)*

### 4.2 Boundary conditions

The experimentation on the wall segment of hemp concrete lasted almost two months, between July 13, 2016 and September 08, 2016. Fig. 8 and Fig. 9 show the measured relative humidity and temperature variations within ambient air at the boundaries of the sample. The external air relative humidity and temperature are found to present a cyclic variation, the mean values recorded for RH is 73.90 % ± 25 % and 20.19°C ± 10°C. The indoor conditions were found to be more stable with mean values of 21.55 °C for the temperature and 58.80 % for the relative humidity.

The solar effect was neglected in the modeling due to the orientation of the studied wall segment, which was completely oriented to the North. Other orientations will be the subject of future research work where the solar heat flux effect may be more important; in this case another term will be added to the equation model in order to refine the simulation and get more precision.

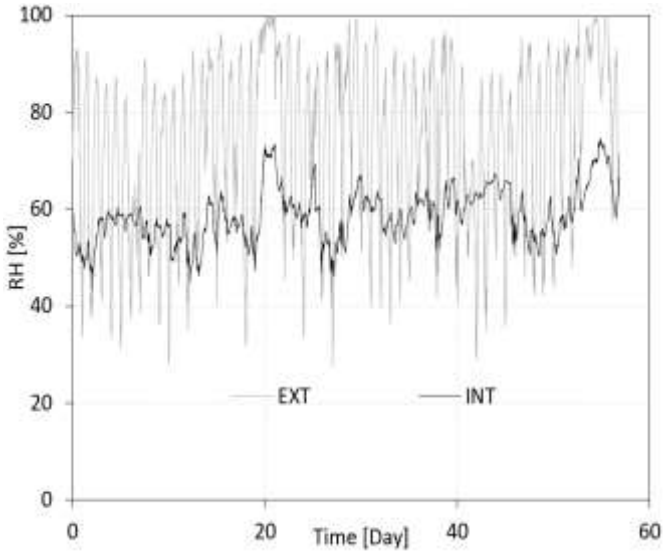


*Fig.8 Measured relative humidity in the ambient air*

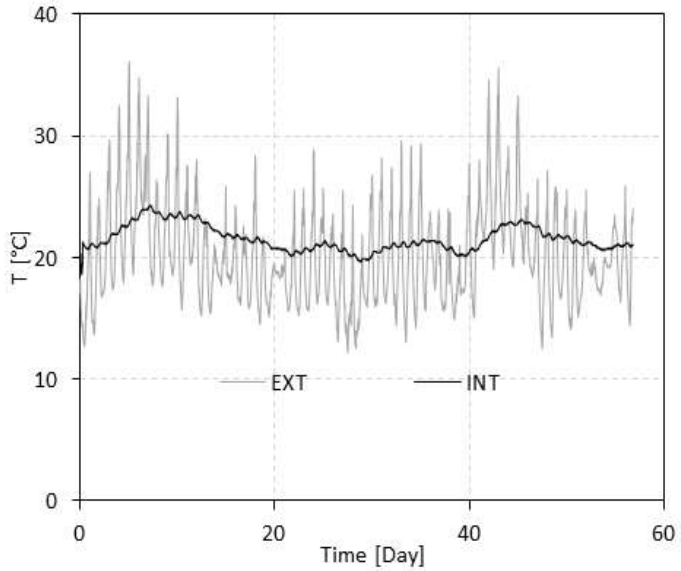


*Fig.9 Measured temperature in the ambient air*

### 4.3 Comparison between simulation and experimentation

The simulations were performed by solving the coupled nonlinear partial differential equations (Eq.1 and Eq.2) in the "PDE Modes" of COMSOL Multiphysics® [40]. The software was chosen for its high flexibility in adding the equations and the boundary conditions. The problem was solved using a 2mm mesh size and a 300s time step which corresponds to the acquisition time step that was used during the experiment. The simulations were implemented with the measured properties of the material obtained by the material characterization experimental setup. The results for humidity variations (measured and simulated data) inside the sample at 2cm, 4cm and 6cm are shown in Fig. (10-11-12). Two segments of 5 days each were chosen to ensure a clear display of data.

A compatibility between the simulated and measured data in terms of kinetic evolution is observed; the simulated and measured curves present similar trends.

The observation of the three graphs shows that the accuracy of the relative humidity is related to the position inside the sample; the local variation of relative humidity at 2 cm present some difference in terms of amplitude, while a higher accuracy is recorded at a depth of 6 cm. The decrease in the accuracy close to the indoor side may be justified by the precision of the boundary conditions logged for the inner side.

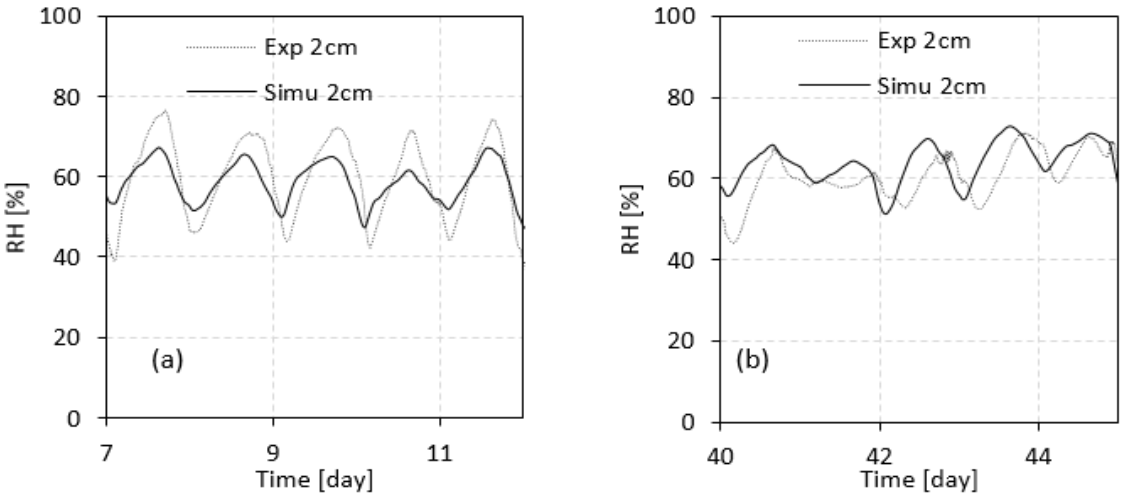


*Fig.10 (a-b) Measured and simulated relative humidity inside the sample at x = 2cm*

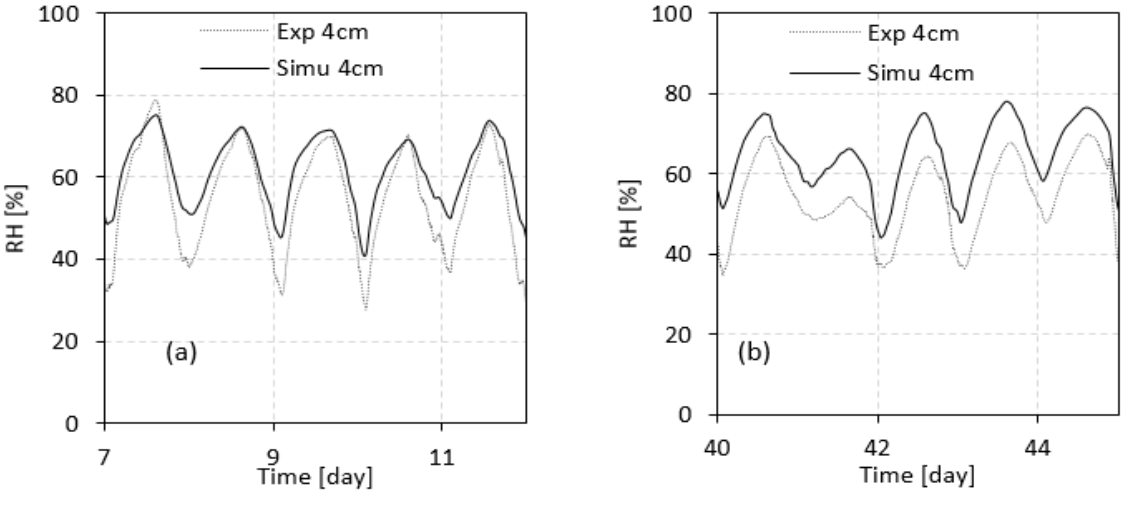


*Fig.11 (a-b) Measured and simulated relative humidity inside the sample at x = 4cm*

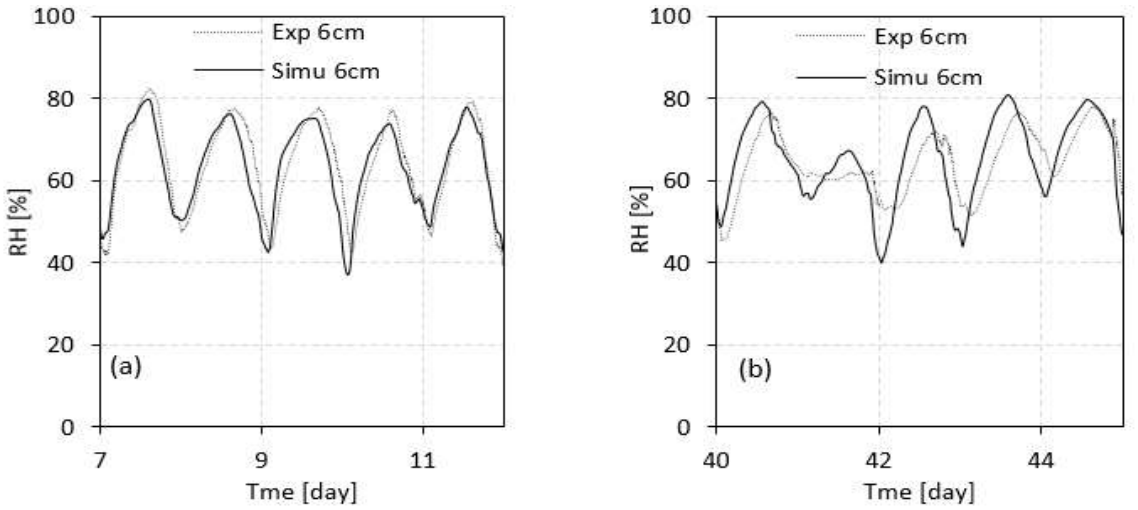


*Fig.12 (a-b) Measured and simulated relative humidity inside the sample at x= 6cm*

The simulated and the measured relative humidity variations during the transient phase at 5 days, 12 days, 17 days, and 26 days are shown Fig. 13. The results show a good agreement and small difference between the measured and simulated values over the thickness of the sample for the different chosen instants.

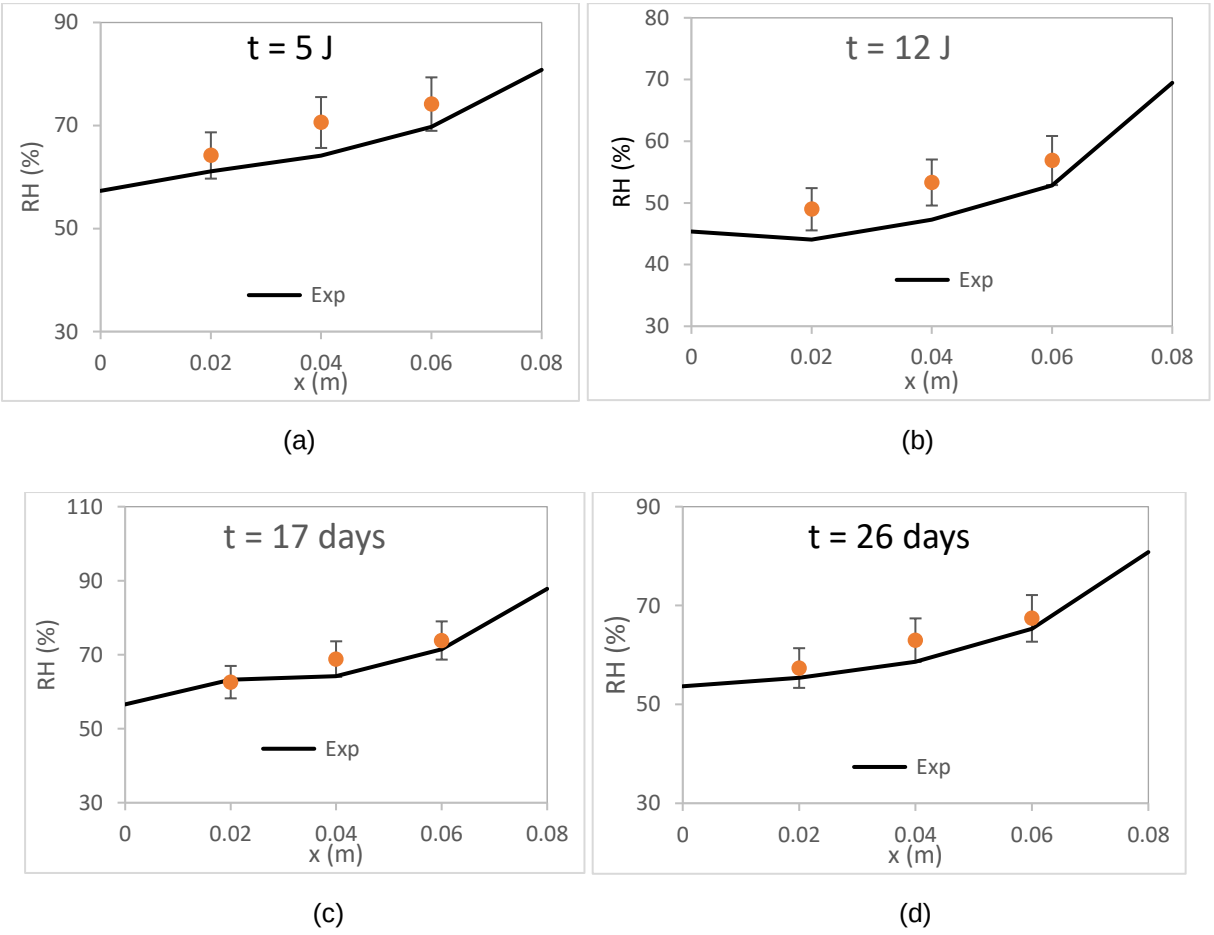


*Fig.13 Measured and simulated relative humidity profiles within the sample at t = 5 days (a), t = 12 days (b), t = 17 days (c), and t = 26 days (d)*

The decrement factors and time lags were evaluated from the humidity curves and expressed in (hh:mm) and (%) for time las and decrement factors respectively. By definition, the term 'decrement factor' refers to the amount by which conditions are moderated by a building element. In other terms, when a temperature (or humidity) peak reaches the outer surface of a building element, the decrement factor represents the amount by which this peak is reduced by the time it reaches the inner surface.

The average decrement values at 2cm, 4cm and 6 cm were respectively: 14%, 20% and 24% and the average time lag values were 2h45min, 3h22min and 5h15min. Fig. 14 presents the histogram of relative humidity decrement factors and time lags for the hemp concrete sample. The results show that the decrement factor and the time lag increase with respect to the thickness, which is usually observed for insulation material.

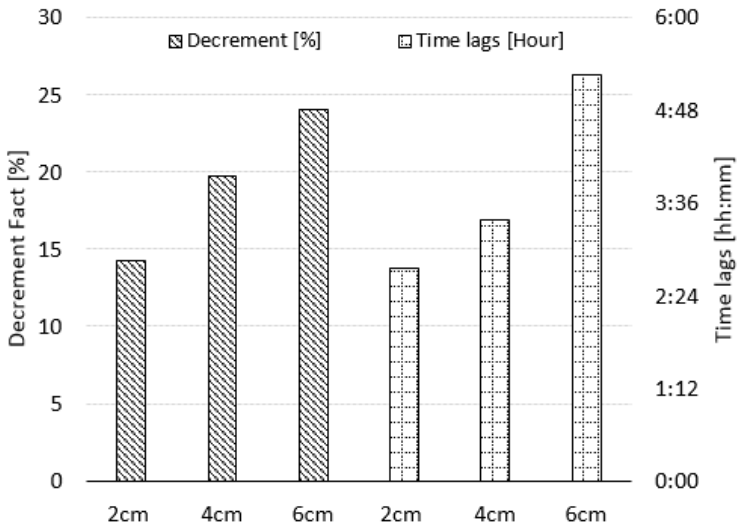


*Fig.14 Decrement factors and time lags evaluated for different thicknesses of hemp concrete*

Fig. 15 to Fig. 17 present measured and simulated variations for temperature within the tested wall segment. Although no perfect match can be observed between the numerical results and the experimental data close to the inner side at a depth of 2cm (Fig 14-a.), the results remain in very good agreement in all the remaining cases. Better agreement was found at x = 4 cm (Fig.16) and at x = 6 cm (Fig. 17) than close to the surface x = 2cm. This slight difference can be caused by the heterogeneity of the material, the uncertainty on the physical properties of the material during the characterization campaign, and the sensor's position and accuracy. Furthermore, the hysteresis effects also present a major factor of discrepancy **[41], [42], [43], [44]**.

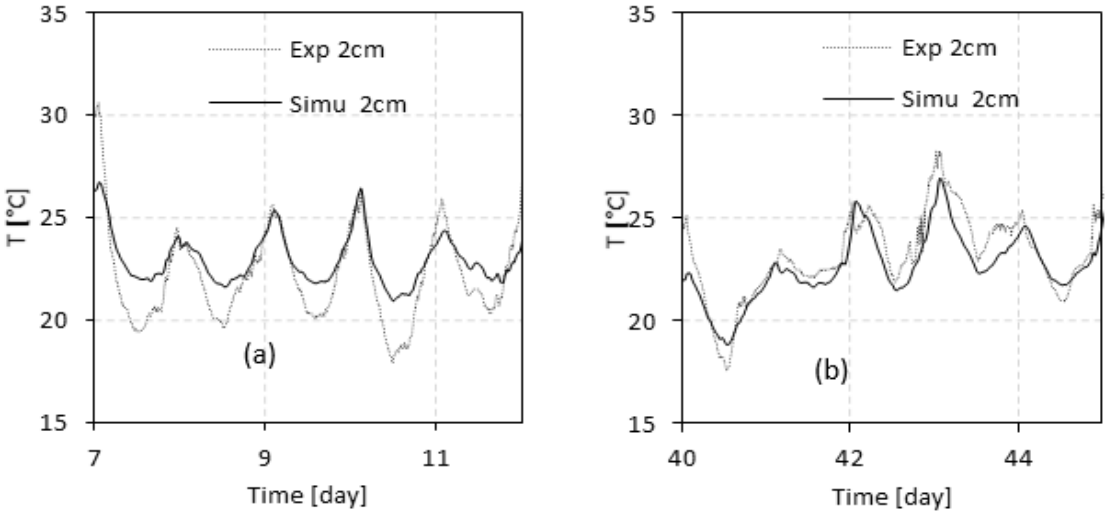


*Fig.15 (a-b) Measured and simulated temperature inside the sample at x = 2cm*

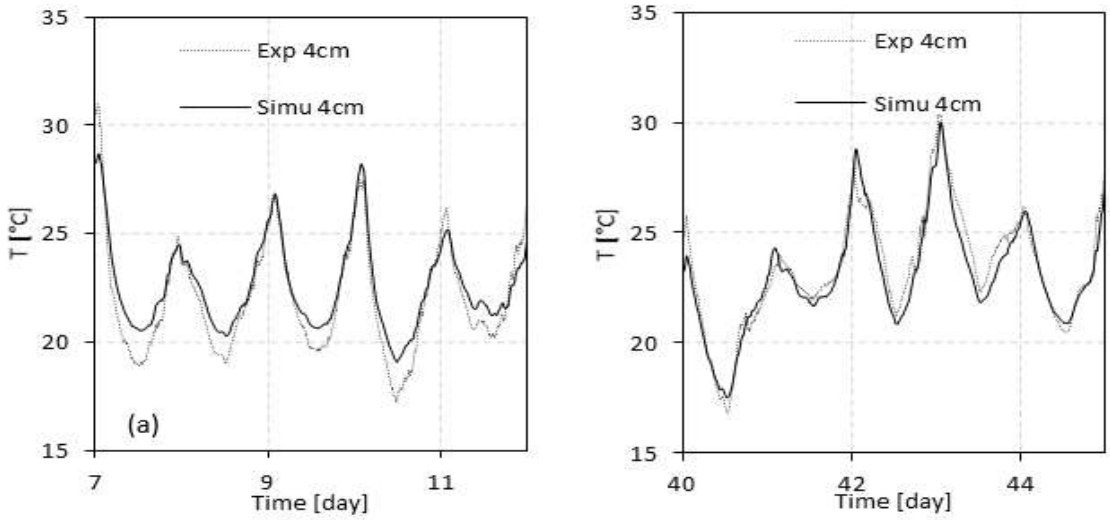


*Fig.16 (a-b) Measured and simulated temperature inside the sample at x = 4cm*

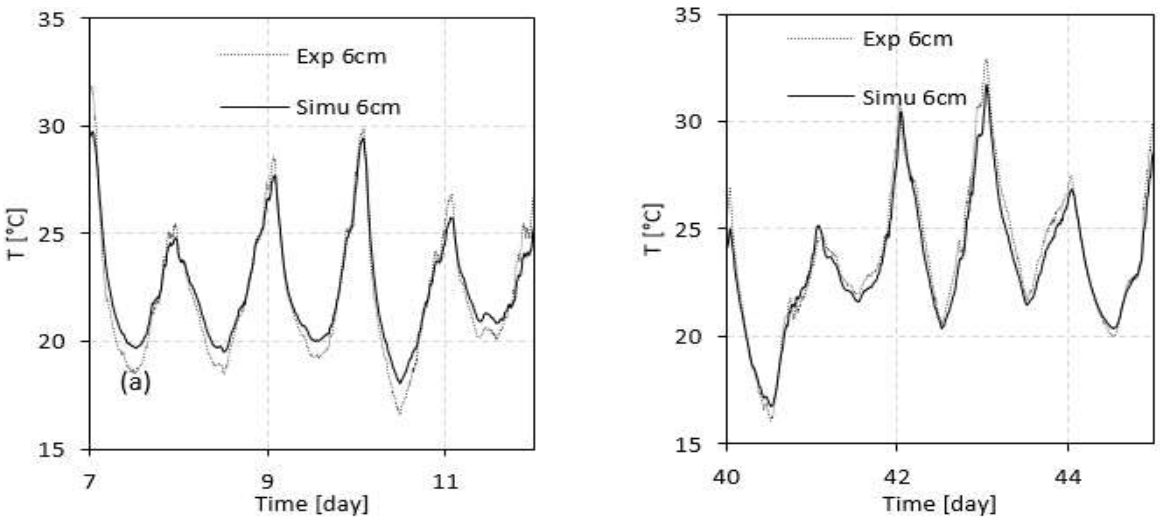


*Fig.17 (a-b) Measured and simulated temperature inside the sample at x = 6cm*

Fig.18 shows the decrement factors (%) and the time lags of temperature. The decrement factors are evaluated, the results are respectively 7% for a thickness of 2 cm, 11.42% for 4cm, and 14.46% for 6 cm. Concerning the time lags the following vales are founded: 1h08, 1h48, 2h23 for 2cm, 4cm and 6cm of thickness. The time lags can be calculated for any material by the formulation (Eq.13).

$$Time\_lags = \frac{P}{2\,\pi}\sqrt{\frac{\pi\,\rho\,C}{\lambda\,P}}\;e \qquad (13)$$

Where e (m) is the material thickness, P is the cycle of temperature variation (hour), ρ is the material density (kg.m$^{-3}$), λ (W.m$^{-1}$.K$^{-1}$) and C (J.kg$^{-1}$.K$^{-1}$) are the thermal conductivity and specific heat respectively. The calculated and experimentally evaluated time lags are plotted in Fig. 18. Because of some practical uncertainty in the experimental results, and the assumptions in the theoretical method, the comparison results have some acceptable differences. Furthermore, the comparison of time lags values of hemp concrete with those founded in the bibliography [45] for a wall of 5cm made of concrete (01:08), polyurethane (00:07), and gypsum (00:53), proves that hemp concrete is more efficient in terms of thermal inertia compared to other conventional materials.

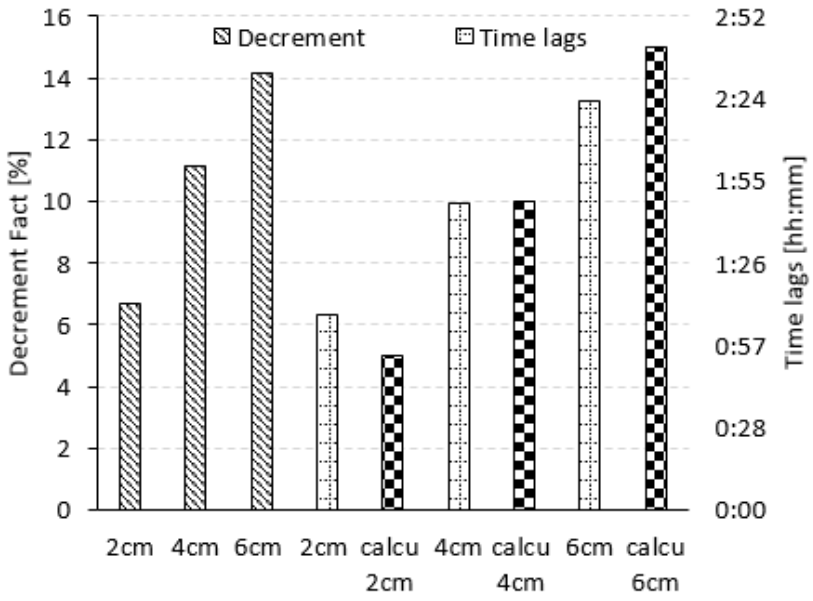


*Fig.18 Decrement factor and time lags evaluated for different thicknesses of hemp concrete*

### 4.4 Sensitivity ANALYSIS

The sensitivity of the sensors was validated by a calibration and balancing test in our laboratory before starting the experimentation and measurement phase. This step was carried out according to the following protocol: the humidity and temperature sensors were placed in the climatic chamber, the interior conditions of the chamber were varied in several ranges and different configurations, isothermal, relative humidity cycles, etc... The aim of these measurements was to validate the data provided by the

sensors using the climatic chamber as reference. In conclusion, the accuracy of the sensors has been widely verified and validated.

To explore the origin of differences observed between the simulated and the measured data, a sensitivity analysis related to the sensors' positions is performed in order to quantify the impact induced by the uncertainty of positions on the local relative humidity and temperature variations. The results presented in Fig. 19 and Fig. 20 show that a positional offset of only 5 mm induces differences of about 4% for the relative humidity and 0.97 °C for the temperature. In view of the material heterogeneity and the difficulty of installing precisely the sensors, the impact of those two parameters justify the slight differences observed between simulated and measured data.

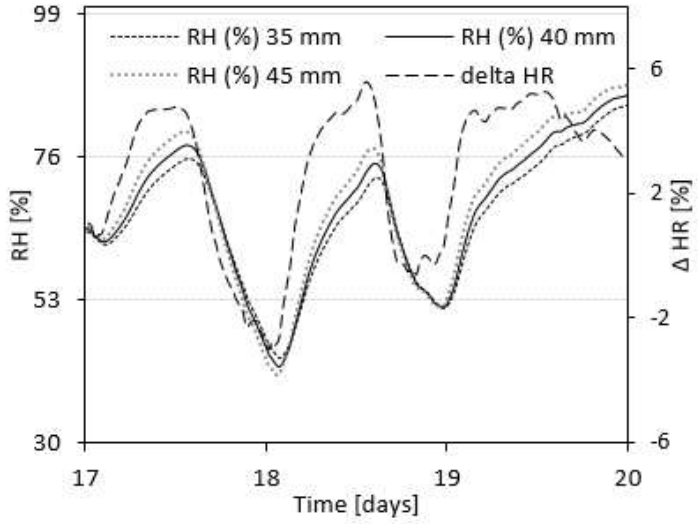


*Fig.19 Influence of sensors positions on the local relative humidity.*

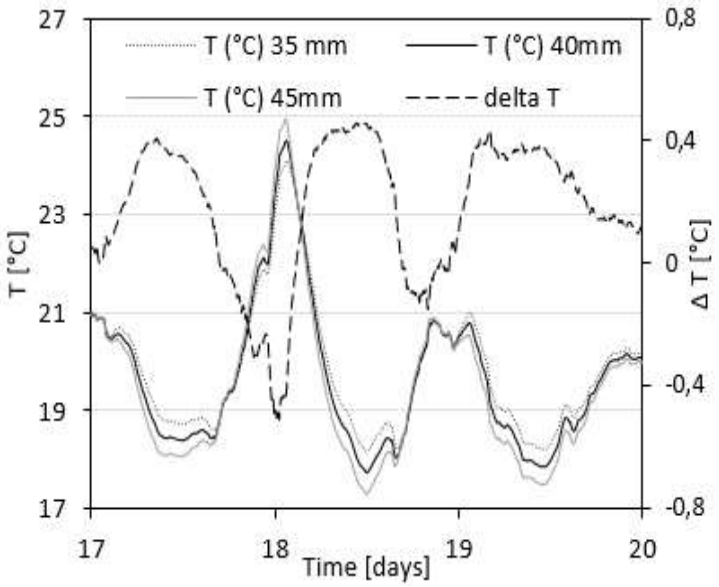


*Fig.20 Influence of sensors positions on the local temperature.*

Furthermore, the sensitivity analysis must be wider and take into account other parameters as materials properties (thermal conductivity, sorption isotherm…).

## 5 MOISTURE BUFFER INVESTIGATION

The Moisture Buffer Value (MBV) characterizes the ability of a material, or a multilayer component, to moderate the air humidity variations. The Japanese Industrial Standard (JIS), the Draft International Standard (DIS) and the Nordtest protocol (NT) all define similar methods based on measurements of mass change of a sample subjected to cyclic variations of relative humidity. In this study, we propose a numerical investigation of hemp concrete subjected to the Nordtest protocol conditions.

The goal of the MBV measurements is to participate in the enrichment of knowledge around hemp concrete, by comparing the behavior of the hemp concrete with respect to the cyclic humidity variations and to determine its ability to moderate these variations. The behavior of hemp concrete is compared to the behavior of other classic materials such as normal concrete, bricks, and glass wool.

The sample conditioned to a specific RH and sealed at all but its normally exposed sides, is alternatingly exposed to a high and a low ambient RH for predefined intervals of time. The sample moisture mass evolution is recorded, and the (MBV) [kg.m$^{-2}$.%RH$^{-1}$] is calculated by:

$$MBV = \frac{m_{max} - m_{min}}{A \,.\, (RH_{high} - RH_{low})} \quad (14)$$

Where $m_{max}$ and $m_{min}$ [kg.m$^{-2}$] are the sample's maximum and minimum moisture mass, obtained in the final stable cycle, A [m$^{-2}$] is the exposed surface of the element's sample, and $RH_{high}$ and $RH_{low}$ [%] are the high/low Relative humidity levels imposed during the test.

The results of the simulated MBV are obtained by simulation with a numerical model for moisture transfer **[46]** . All simulations are isothermal with temperatures constant at 23 °C. The model is presented by Eq.15, and the associated boundary conditions is expressed by the Eq.16.

$$\frac{\partial w}{\partial t} = \nabla( \delta_p(P_v) \nabla P_v) \quad (15)$$

$$G_s = \beta( P_{vi} - P_{vi} ) \quad (16)$$

with w [kg.m$^{-3}$] the moisture content, t [s] the time, $\delta_p$ [s] the water vapor permeability, $p_v$ [Pa] the vapor pressure, $G_s$ [kg.m$^{-2}$.s$^{-1}$] the vapor exchange flux, β [s.m$^{-1}$] the surface mass transfer coefficient, and p $P_{vi}$, $P_{vs}$ [Pa] the interior/surface partial vapor pressure. The Nordtest protocol and the input parameters used in the simulation are reported in Table 2.

Table 2- MBV Simulation parameters

| Protocol Nordtest | Values |
|---|---|
| RH levels (high/low) [%] | 75/33 |

| | |
|---|---|
| Time intervals [h] | 8/16 |
| Surface transfer coeff [s/m] | $10^{-8}$ / $300.100^{-8}$ |
| Sample thickness [cm] | 10 |

Ten cycles have been simulated and the MBV is determined based on the results for the last day. The specimen was supposed to be at least 10 cm thick in order to avoid the moisture penetration depth effect for daily humidity variations. The predicted moisture content evolution is presented in Fig.21. The surface transfer coefficient values varied between $1.10^{-8}$ s.m$^{-1}$ and $3.10^{-6}$ s.m$^{-1}$. Tab. 2 gives an overview of the calculated MBV's of hemp concrete for the different surface transfer coefficients.

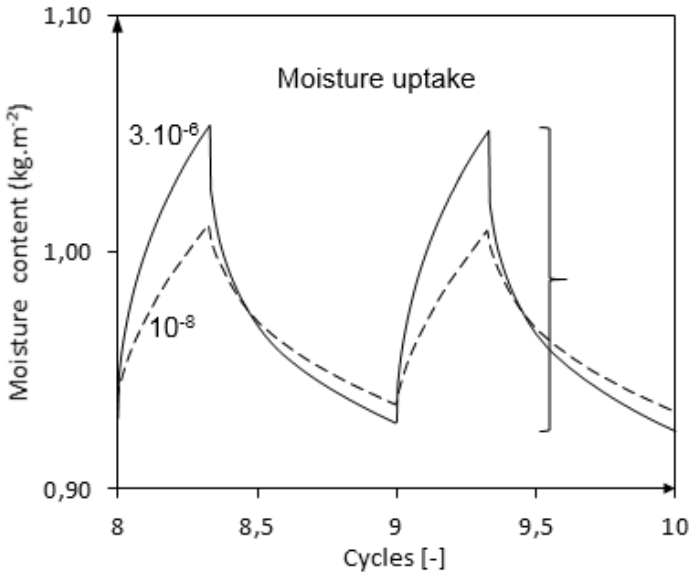


*Fig.21 Simulated moisture content evolution*

The hemp concrete MBV values were respectively 1.82 kg.m$^{-2}$.%RH$^{-1}$ and 3.02 kg.m$^{-2}$.%RH$^{-1}$ for surface transfer coefficient values of $1.10^{-8}$ s.m$^{-1}$ and $3.10^{-6}$ s.m$^{-1}$. These values are in perfect agreement with the results of **[47]** where the average MBV for a hemp concrete wall varied between 1.99 kg.m$^{-2}$.%RH$^{-1}$ and 2.51 kg.m$^{-2}$.%RH$^{-1}$. The relative difference of 39% can be explained by the fact that the hemp concrete is a vapor open material with a high moisture capacity.

Tab.2 MBV calculated for different β coefficients.

| Hemp concrete | β $10^{-8}$ | β $300.100^{-8}$ |
|---|---|---|
| MBV [kg.m$^{-2}$.%RH$^{-1}$] | 1.82 | 3.02 |

The determined MBV values of hemp concrete classifies the material under the category of good or even excellent humidity regulator regarding the classification of Nordtest Project (Fig.22). Moreover, the comparison of these values with those given in the Nordtest Project shows that the hemp concrete is a

much better hygroscopic regulator than cellular concrete (MBV = 1.04 kg.m$^{-2}$.%RH$^{-1}$), plaster (MBV = 0.64 kg.m$^{-2}$.%RH$^{-1}$) and cement concrete (MBV = 0.38 kg.m$^{-2}$.%RH$^{-1}$).

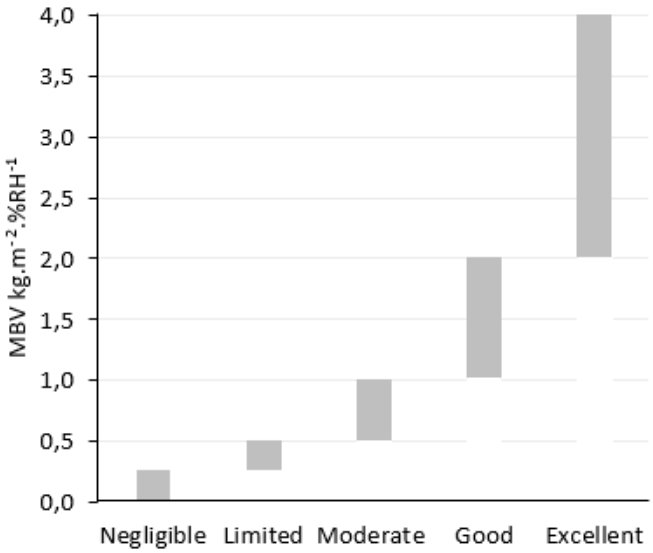


*Fig.22 Nordtest classification of MBV Project [36]*

## 6 CONCLUSION

Although more efforts are still needed to learn more about its hygrothermal behavior. For this purpose, an experimental study was performed in real weather conditions by instrumenting a hemp concrete wall segment with temperature and humidity sensors at its both exposed faces and from inside. The wall segment was exposed to outside weather conditions from one side and to laboratory indoor conditions from the other side.

The material's thermophysical properties were first evaluated experimentally and then used as input parameters in the numerical adopted model describing heat and mass transfer.

The numerical results were in a good agreement with the experimental measurements. Generally, the local variations of temperature and relative humidity were modeled with high accuracy over the wall thickness; a slight difference between the simulated and measured data was observed at a depth of 2cm. For this reason, a sensitivity analysis was carried out to quantify the impact on sensors positions uncertainty.

To study the efficiency of hemp concrete in regulating the ambient humidity, a numerical investigation of the Moisture Buffer Value was performed for the extreme high/low values of surface film coefficients.

From those results and according the Nordtest classification, the hemp concrete can be classified between good and excellent humidity regulator materials. One can conclude that, even if the hemp concrete presents a thermal conductivity higher than other conventional insulation materials, its strong humidity regulation potential as well as dynamic hygrothermal performance (time lag and decrement factor) make it a favored choice to be integrated in energy efficient building envelopes.

The hygrothermal performance of hemp concrete was demonstrated in the real building conditions in this study; however, other tests must be conducted in multilayer common case walls to investigate its potential integration as building layer element in real scenarios.

After comparing the ability of hemp concrete to moderate the ambient humidity conditions and investigating its thermal characteristics with respect to conventional building materials such as rock wool and glass wool, the hemp concrete can be considered as an efficient bio-based material in building envelope.

In the future up-coming studies, a more complete investigation will be carried out for hemp concrete in a multi-layered wall with different configurations, in order to identify the interaction of hemp concrete with other materials and to put forward its performances in a more comprehensive context.

## REFERENCES


[1] O. F. Osanyintola and C. J. Simonson, “Moisture buffering capacity of hygroscopic building materials: experimental facilities and energy impact,” *Energy Build.*, vol. 38, no. 10, pp. 1270–1282, 2006.

[2] D. Peñaloza, M. Erlandsson, and A. Falk, “Exploring the climate impact effects of increased use of bio-based materials in buildings,” *Constr. Build. Mater.*, vol. 125, pp. 219–226, Oct. 2016.

[3] M.P.Sáez-Pérez, M.Brümmer, J.A.Durán-Suárez, “A review of the factors affecting the properties and performance of hemp aggregate concretes”, Journal of Building Engineering, Volume 31, September 2020

[4] G.Delannoy, S.Marceau, P.Glé, E.Gourlay, M.Guéguen-Minerbe, S.Amziane, F.Farcas, “Durability of hemp concretes exposed to accelerated environmental aging”, *Construction and Building Materials*, Volume 252, no. 119043, August 2020.

[5] F. Benmahiddine, F. Bennai, R. Cherif, R. Belarbi, A. Tahakourt, K. Abahri, “Experimental investigation on the influence of immersion/drying cycles on the hygrothermal and mechanical properties of hemp concrete”, *Journal of Building Engineering*, no. 101758, August 2020

[6] R. Holopainen, P. Tuomaala, P. Hernandez, T. Häkkinen, K. Piira, and J. Piippo, “Comfort assessment in the context of sustainable buildings: Comparison of simplified and detailed human thermal sensation methods,” *Building and Environment*, pp. 60–70, Sep-2013.

[7] A. Limam, A. Zerizer, D. Quenard, H. Sallee, and A. Chenak, “Experimental thermal characterization of bio-based materials (Aleppo Pine wood, cork and their composites) for building insulation,” *Energy Build.*, vol. 116, pp. 89–95, Mar. 2016.

[8] O. Vololonirina, M. Coutand, and B. Perrin, “Characterization of hygrothermal properties of wood-based products – Impact of moisture content and temperature,” *Constr. Build. Mater.*, vol. 63, pp. 223–233, Jul. 2014.

[9] T. M. Tuzcu, “Hygro-Thermal Properties of Sheep Wool Insulation,” Civil Engineering Faculty Delft University of Technology, 2007.

[10] F. Collet and S. Pretot, “Experimental investigation of moisture buffering capacity of sprayed hemp concrete,” *Constr. Build. Mater.*, vol. 36, pp. 58–65, Nov. 2012.

[11] M. Palumbo, A. M. Lacasta, N. Holcroft, A. Shea, and P. Walker, “Determination of hygrothermal parameters of experimental and commercial bio-based insulation materials,” *Constr. Build. Mater.*, vol. 124, pp. 269–275, Oct. 2016.

[12] C. Bories, E. Vedrenne, A. Paulhe-Massol, G. Vilarem, and C. Sablayrolles, “Development of porous fired clay bricks with bio-based additives: Study of the environmental impacts by Life Cycle Assessment (LCA),” *Constr. Build. Mater.*, vol. 125, pp. 1142–1151, Oct. 2016.

[13] S. Elfordy, F. Lucas, F. Tancret, Y. Scudeller, and L. Goudet, “Mechanical and thermal properties of lime and hemp concrete (‘hempcrete’) manufactured by a projection process,” *Constr. Build*, Oct. 2008.

[14] A. D. Tran Le, C. Maalouf, T. H. Mai, E. Wurtz, and F. Collet, “Transient hygrothermal behaviour of a hemp concrete building envelope,” *Energy Build.*, vol. 42, no. 10, pp. 1797–1806, Oct. 2010.

[15] D. Lelievre, T. Colinart, and P. Glouannec, “Hygrothermal behavior of bio-based building materials including hysteresis effects: Experimental and numerical analyses,” *Energy Build.*, vol. 84, pp. 617–627, Dec. 2014.

[16] A. Shea, M. Lawrence, P. Walker, "Hygrothermal performance of an experimental hemp–lime building", Construction and Building Materials, Vol. 36, pp. 270-275 November 2012.

[17] D. C. Ngo, J. Saliba, N. Saiyouri, Z. M. Sbartaï, “Design of a soil concrete as a new building material – Effect of clay and hemp proportions”, *Journal of Building Engineering*, Vol. 32, no. 101553, November 2020.

[18] T. Jami, S. R. Karadea, L. P. Singh, “A review of the properties of hemp concrete for green building applications, Journal of Cleaner Production”, *Journal of Cleaner Production*, Vol. 239, no. 117852, December 2019.

[19] H. Viitanen *et al.*, “Moisture and Bio-deterioration Risk of Building Materials and Structures,” *J. Build. Phys.*, vol. 33, no. 3, pp. 201–224, Jan. 2010.

[20] A. V. Arundel, E. M. Sterling, J. H. Biggin, and T. D. Sterling, “Indirect Health Effects of Relative Humidity in Indoor Environments,” *Environmental Health Perspectives*, p. 351–361,.

[21] H. Rafidiarison, R. Rémond, and E. Mougel, “Dataset for validating 1-D heat and mass transfer models within building walls with hygroscopic materials,” *Building and Environment*, pp. 356–368, 14-Mar-2015.

[22] S. Geving, E. Lunde, and J. Holme, “Laboratory Investigations of Moisture Conditions in Wood Frame Walls with Wood Fiber Insulation,” *Energy Procedia*, vol. 78, pp. 1455–1460, Nov. 2015.

[23] C. Maalouf, A. D. T. Le, S. B. Umurigirwa, M. Lachi, and O. Douzane, “Study of hygrothermal behaviour of a hemp concrete building envelope under summer conditions in France,” *Energy Build.*, vol. 77, pp. 48–57, Jul. 2014.

[24] M. Rahim, O. Douzanea, D. Tranle, G. Promis, and T. Langlet, “Experimental investigation of hygrothermal behavior of two bio-based building envelopes,” *Energy Build.*, Jan. 2017.

[25] J. R. Philip and D. A. De Vries, “Moisture Movement in Porous Materials under Temperature Gradients,” *Transactions, American Geophysical Union*, pp. 222–232, Apr-1957.

[26] A. V. Luikov, “System of differential equation of heat and mass transfer in capillary porous bodies,” *International Journal of Heat and Mass Transfer*, pp. 1–14, 1957.

[27] S. Whitaker, “Simultaneous Heat, Mass, and Momentum Transfer in Porous Media: A Theory of Drying,” *Advances In Heat Transfer,* 1977.

[28] H. Kunzel, “Simultaneous heat and moisture transport in building components: one- and two dimensional calculation using simple parameters,” IRB Verlag Suttgart, 1995.

[29] H. Janssen, B. Blocken, and J. Carmeliet, “Conservative modelling of the moisture and heat transfer in building components under atmospheric excitation,” *Int. J. Heat Mass Transf.*, vol. 50, no. 5–6, pp. 1128–1140, Mar. 2007.

[30] A. Zaknoune, · P. Glouannec, and P. Salagnac, “Identification of the Liquid and Vapour Transport Parameters of an Ecological Building Material in Its Early Stages,” *Transport in Porous Media*, pp. 589–613, 2013.

[31] Béton de Chanvre, “http://chanvribloc.com/le-beton-de-chanvre/.”

[32] NF EN 12664, “Thermal performance of building materials and products. Determination of thermal resistance by means of guarded hot plate and heat flow meter methods. Dry and moist products of medium and low thermal resistance,” pp. 75–225, 2001.

[33] “NF EN ISO 12571 Hygrothermal performance of building materials and products- Determination of hygroscopic sorption properties,” 25-Oct-2013.

[34] E. Guggenheim, “Application Of Statistical Mechanics,” *Oxford University Press*, 1966.

[35] Von H. J. de Boer., “The Dynamical Character of Adsorption,” *Oxford University Press*, 1953.

[36] (2001) NF EN ISO 12572 Hygrothermal performance of building material and products Determination of water vapour transmission properties.

[37] T. Colinart, D. Lelievre, and P. Glouannec, “Experimental and numerical analysis of the transient hygrothermal behavior of multilayered hemp concrete wall,” *Energy Build.*, vol. 112, pp. 1–11, Jan. 2016.

[38] F. Collet and S. Pretot, “Thermal conductivity of hemp concretes: Variation with formulation, density and water content,” *Constr. Build. Mater.*, vol. 65, pp. 612–619, Aug. 2014.

[39] “http://graphteccorp.com/instruments/gl82/index.html.”

[40] “Comsol Multiphysics,” http://www.comsol.com/products/multiphysics/. .

[41] X. Zhang, W. Zillig, H.M. Künzel, C. Mitterer, X. Zhang, Combined effects of sorption hysteresis and its temperature dependency on wood materials and building enclosures-part II: Hygrothermal modeling, Building and Environment. 106 (2016) 181–195. https://doi.org/10.1016/j.buildenv.2016.06.033.

[42] Y. Aït Oumeziane, S. Moissette, M. Bart, F. Collet, S. Pretot, C. Lanos, Influence of hysteresis on the transient hygrothermal response of a hemp concrete wall, *Journal of Building Performance Simulation*. 10 (2017) 256–271. https://doi.org/10.1080/19401493.2016.1216166.

[43] T. Alioua, B. Agoudjil, N. Chennouf, A. Boudenne, K. Benzarti, Investigation on heat and moisture transfer in bio-based building wall with consideration of the hysteresis effect, *Building and Environment*. 163 (2019) 106333. https://doi.org/10.1016/j.buildenv.2019.106333.

[44] N. Reuge, F. Collet, S. Pretot, S. Moisette, M. Bart, O. Style, A. Shea, C. Lanos, Hygrothermal effects and moisture kinetics in a bio-based multi-layered wall: Experimental and numerical studies, *Construction and Building Materials*. 240 (2020) 117928.

https://doi.org/10.1016/j.conbuildmat.2019.117928.

[45] H. Asan, “Numerical computation of time lags and decrement factors for different building materials,” *Build. Environ.*, vol. 41, no. 5, pp. 615–620, May 2006.

[46] H. Janssen, B. Blocken, and J. Carmeliet, “Conservative modelling of the moisture and heat transfer in building components under atmospheric excitation,” *Int. J. Heat Mass Transf.*, vol. 50, no. 5–6, pp. 1128–1140, Mar. 2007.

[47] F. Collet and S. Pretot, “Variation de la capacité hydrique tampon de bétons de chanvre en fonction de la formulation,”
*Actes du 1er Congrès écobat Sciences & Techniques, écobat Sciences & Techniques*, 2012, pp. 140–148.